Eco-friendly Synthesis of $SrBi_4Ti_{3,95}Fe_{0,05}O_{15}$ via Molten Salt Method

Rizki Fitriana Dewi(✉) and Anton Prasetyo

Department of Chemistry, Faculty Science and Technology, Universitas Islam Negeri Maulana Malik Ibrahim Malang, Jalan Gajayana 50, Malang 65144, Indonesia
rizkifitriana808@gmail.com

Abstract. The molten salt synthesis has been known as an eco-friendly synthesis method because it does not produce hazardous waste and also, there is no requirement for a high calcination temperature. In this research, we synthesized $SrBi_4Ti_{3.95}Fe_{0.05}O_{15}$ photocatalytic material via the molten salt method using NaCl, KCl, and NaCl/KCl salt. The diffractogram sample showed that $SrBi_4Ti_{3.95}Fe_{0.05}O_{15}$ product obtained using KCl salt had successfully obtained with no impurities, but the $SrBi_4Ti_{3.95}Fe_{0.05}O_{15}$ product synthesized using NaCl salt has found an impurities phase of $Bi_4Ti_3O_{12}$ and TiO_2 (brookite). $SrCO_3$ impurities was also found on $SrBi_4Ti_{3.95}Fe_{0.05}O_{15}$ product that was synthesized using NaCl/KCl salt. The micrographs showed that the sample's morphology is plate-like and still found agglomeration. The results of the Kubelka-Munk calculation showed that the $SrBi_4Ti_{3.95}Fe_{0.05}O_{15}$ has a band gap energy of about 2.32–2.55 eV.

Keywords: Molten salt synthesis · NaCl · KCl · NaCl/KCl · $SrBi_4Ti_{3.95}Fe_{0.05}O_{15}$

1 Introduction

As well known, the molten salt synthesis method (MSS) have some advantage, such as being cheap, efficient, and eco-friendly, requiring a lower temperature, and no hazardous waste [1]. Therefore MSS is known as an eco-friendly synthesis method. Many researchers have used MSS to synthesize various metal oxide compounds, such as compounds with perovskite and Aurivillius structures. $SrBi_4Ti_4O_{15}$ (SBT) is a member of a four-layer Aurivillius compound that was reported to have photocatalytic properties with band gap energy of about 3.0 eV (~420 nm) [2]. The transition metal doped such as Fe^{3+}, Er^{3+}, and V^{4+} in SBT is a strategy to decrease its band gap energy. Thus photocatalyst SBT can work in a wider visible light [3]. The use of Fe metal as doping in compounds with the Aurivillius structure has been carried out by Liu, *et al.* [4] and reporting can reduce its band gap energy [5].

The plate-like (sheet) particle of Aurivillius structure was reported to have good activity photocatalytic [6]. It indicates that if we can synthesized Aurivillius compound with plate-like/sheet morphology so that will give advantage in photocatalyst applied.

E. Susanti et al. (Eds.): ICGT 2022, AER 221, pp. 118–126, 2023.
https://doi.org/10.2991/978-94-6463-148-7_13

Many researchers reported successful synthesis of SBT using the molten salt method and obtained plate-like morphology particle [7]. Sari, *et al.* synthesized the V-doped SBT through KCl molten salt method and obtained the plate-like particle with less agglomeration while V-doping caused the band gap energy decrease [8].

There are many factor which influence to MSS such as temperature and time synthesis, ratio molar product to salt, and salt type [9]. Chang, et al. succeeded in synthesizing plate-like SBT using different salt i.e. NaCl, Na_2SO_4, KCl, and K_2SO_4. They suggested that the salt type affected to phase of the product and the size particle. Morphology particle of product also affected by salt type in the molten salt method [10]. Liu, *et al.* synthesized $Y_{0.95}Sm_{0.02}Eu_{0.03}VO_4$ compound using MSS and obtained spherical particle shape by KCl molten salt, meanwhile a regular rod-like particle is formed by using NaCl molten salt. The differentiation morphology indicated to come from the differences of environmental reaction condition [11]. Therefore, in this research we synthesized Fe doped SBT ($SrBi_4Ti_{3.95}Fe_{0.05}O_{15}$) prepared by MSS and used different salt type was NaCl, KCl, and KCl/KCl, and studied using (a) X-ray diffraction technique (XRD), (b) scanning electron microscopy (SEM), and (c) ultraviolet-visible diffuse reflectance spectroscopy (UV-Vis DRS).

2 Method

2.1 Materials

In this research used: (Bi_2O_3) (Sigma-Aldrich, 99.9%), Fe_2O_3 (Sigma-Aldrich, 99.9%), $SrCO_3$ (Sigma-Aldrich, 99.9%), TiO_2 (Sigma-Aldrich, 99.9%), NaCl (Merck, 99.9%), KCl (Merck, 99.9%), $AgNO_3$ (Aldrich, larutan 2,5%), acetone, and aquadest.

2.2 Synthesis of $SrBi_4Ti_{3.95}Fe_{0.05}O_{15}$

$SrBi_4Ti_{3.95}Fe_{0.05}O_{15}$ compound was prepared by molten salt method using NaCl, KCl, and NaCl/KCl (molar ratio 1:1). The target mass of all samples are 3 gram. All precursors were weighed stoichiometrycally and grinded in a mortar agate for 1 hour with each salts in a salt-to-oxide weight ratio of 1:7. Acetone was added during grinding process to homogenize mixture. The mixture was put into an alumina crucible and calcined at a temperature of 825 and 850 °C for 6 hours. Then, the samples were cooled to room temperature and washed with warm water to remove the salts. The filtrate was tested by $AgNO_3$ to make sure that the salt is gone. Finally, the obtained powders were dried in oven at 90 °C for 6 h.

2.3 Characterization

The sample phase of the product was characterized by XRD with Cu Kα radiation 40 kV and 15 mA in the range $2\theta = 10–80°$. The diffractogram of product was compared by the Inorganic Crystal Structure Database (ICSD) number 96608 and refined using Rietica software with Le-Bail method. The particle morphology and elemental composition of product were characterized by SEM-EDS. The reflectance spectrum was determined by UV-Vis DRS instrument, then the obtained spectrum was calculated using the Kubelka-Munk equation to get the band gap energy.

3 Result and Discussion

The diffractogram of $SrBi_4Ti_{3.95}Fe_{0.05}O_{15}$, were shown in Fig. 1. All peaks in the XRD pattern can be indexed with the SBT standard database ICSD No. 96608 and it shows the characteristical peaks of the product $SrBi_4Ti_{3.95}Fe_{0.05}O_{15}$ at 2θ (°) = 17.3, 23.2, 30.4, 32.9, 39.7, 47.16, 52.3, and 57.15. The product that synthesized using NaCl and mixture (NaCl/KCl) have an additional peaks at 2θ (°) = 30.64, 15.95, and 35.17. The identification indicate that there is an impurities comes from the precursors that are TiO_2 (30.64°) and $SrCO_3$ (15.95°), also it formed a new phase of $Bi_4Ti_3O_{12}$ (35.17°). The presence of impurities while using NaCl and NaCl/KCl salts indicates that the formation of the synthesized phase was influenced by salt type. The salt flux in molten salt synthesis acts as a reaction medium that facilitates ionic diffusion between reactants (precursors) and then reacts between precursors [1]. The reactants dissolved in the molten salt will diffuse to the surface of the less soluble reactants and form a product [12]. The solubility of the reactant to salt affected the rate of diffusion. The presence of precursors as impurities indicates that the reaction is not complete.

Figure 2 showed the diffractogram peak of $SrBi_4Ti_{3.95}Fe_{0.05}O_{15}$ at $2\theta = 30.4°$ and can be seen the peak position shifting to a larger 2θ. It indicated the local structural changes; as a result, the Fe dopant succeeded in substituting small partially Ti. The size of the crystal lattice becomes smaller because the ionic radii of Fe^{3+} (0.064 nm) have a smaller size than the ionic radii of Ti^{4+} (0.068 nm). In addition, the sharpness of all peaks in the diffractogram showed that the Fe dopant did not influence the crystallinity degree of $SrBi_4Ti_{3.95}Fe_{0.05}O_{15}$.

The diffractogram of $SrBi_4Ti_{3.95}Fe_{0.05}O_{15}$ synthesized using KCl salt was refined using the Le-Bail method. The refinement process using standard data of $SrBi_4Ti_4O_{15}$ (ICSD No. 96608) with an orthorhombic structure, $A2_1am$ space group, cell parameters a

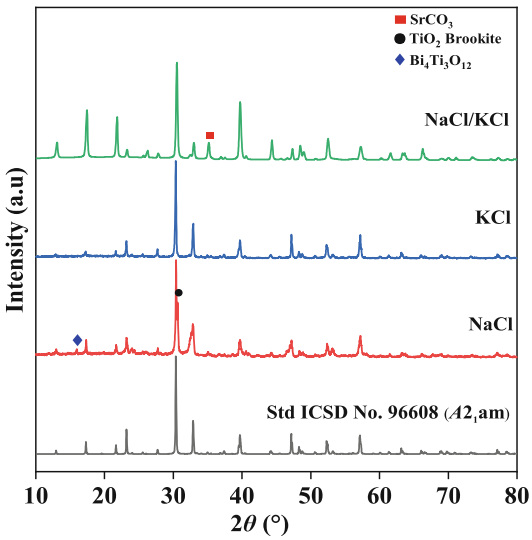

Fig. 1. The diffractogram of SrBi4Ti3.95Fe0.05O15

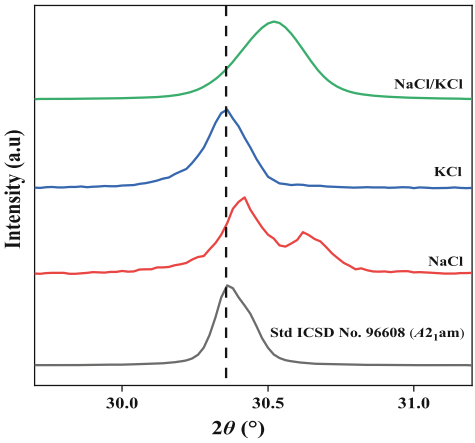

Fig. 2. The diffractogram peaks shifting of $SrBi_4Ti_{3.95}Fe_{0.05}O_{15}$ at $2\theta = 30{,}4°$

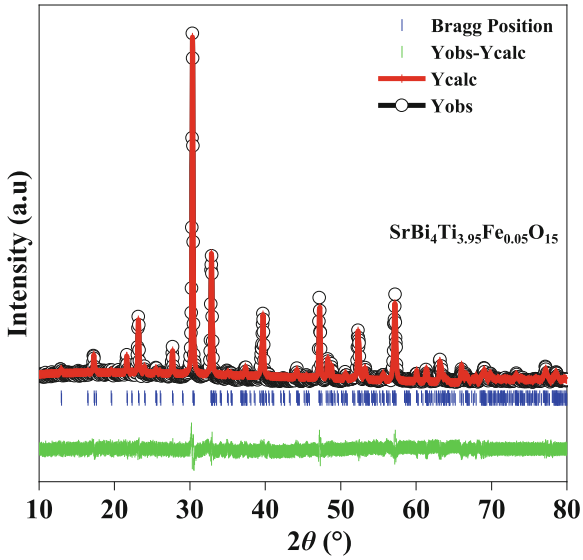

Fig. 3. The refinement plot of $SrBi_4Ti_{3.95}Fe_{0.05}O_{15}$ synthesized using KCl.

$= 5.4510, b = 5.4415, c = 41.0233$, and $\alpha = \beta = \gamma = 90°$. Figure 3 showed the refinement plot, and the results of $SrBi_4Ti_{3.95}Fe_{0.05}O_{15}$ were summarized in Table 1. The results showed that the residual profile value (R_p) is 13.93%, the residual weight profile (R_{wp}) is 9.37%, and the goodness of fit (χ^2) is 0.1334. Based on the values obtained, the diffractogram of $SrBi_4Ti_{3.95}Fe_{0.05}O_{15}$ has good accordance with the standard data.

Figure 4 showed the morphology of $SrBi_4Ti_{3.95}Fe_{0.05}O_{15}$ compound. The morphology particle sample was plate-like and had an agglomeration. The plate-like morphology with a more regular shape is adopted by the sample synthesized using KCl. Meanwhile,

Table 1. Crystallographic data for SrBi4Ti3.95Fe0.05O15

Parameter	**$SrBi_4Ti_{3,95}Fe_{0,05}O_{15}$-KCl**
Crystal System	Orthorombic
Space Group	$A2_1am$
Azimetric Units (Z)	4
a (Å)	5.451000
b (Å)	5.441500
c (Å)	41.023300
Cell Volume ($Å^3$)	1216.817505
R_p (%)	13.93
R_{wp} (%)	9.37
GoF ($\chi 2$)	0.1334

the sample synthesized by NaCl/KCl has a thinner, more extended particle and less agglomeration. It indicates that the morphology particle of the product was affected by salt type. The MSS method has two main stages in the particle growth process; there are (a) nucleation and (b) crystal growth [13]. If the crystal growth rate is faster than nucleation, a larger particle will be produced [14]. The particle morphology of $SrBi_4Ti_{3.95}Fe_{0.05}O_{15}$ is influenced by the solubility of the precursors (reactant) to the salt. The reactants less soluble in the molten salt will have formed the product phase at first and caused agglomeration on the surface particles. The over-substitute of Fe dopant also caused an agglomeration and affected the irregular plate-like morphology that $SrBi_4Ti_{3.95}Fe_{0.05}O_{15}$ adopted. The particle can hold on to the adopted morphology and reduce the particle size if the dopant is substituted correctly. Table 2 tabulated the product's constituent elements: strontium, bismuth, titanium, iron, and oxygen. Fe dopant has succeeded in replacing, but it exceeded the actual amount of about 0.21%.

Figure 5 showed the DRS Spectrum of $SrBi_4Ti_{3.95}Fe_{0.05}O_{15}$ and can be seen the compound can work in the wavelength of 380–450 nm. The plot Tauc was calculated by Kubelka-Munk equation of $SrBi_4Ti_{3.95}Fe_{0.05}O_{15}$. Figure 6 showed the reflectance of $SrBi_4Ti_{3.95}Fe_{0.05}O_{15}$ plotted by the Kubelka-Munk equation (y axis) against the photon energy (x axis). The band gap energies of $SrBi_4Ti_{3.95}Fe_{0.05}O_{15}$ are tabulated in Table 3, and all samples have band gap energy below 3.00 eV. The decreased band gap energy indicated that Fe dopant increases the absorption of $SrBi_4Ti_{3.95}Fe_{0.05}O_{15}$ into the visible light region. The dopant caused a possible change of electronic transition from Bi-6s + O-2p (VB) to Ti-3d (CB) orbitals to Bi-6s + O-2p (VB) to Fe-3d (CB) orbitals with lower band gap energy than the pure compound [15].

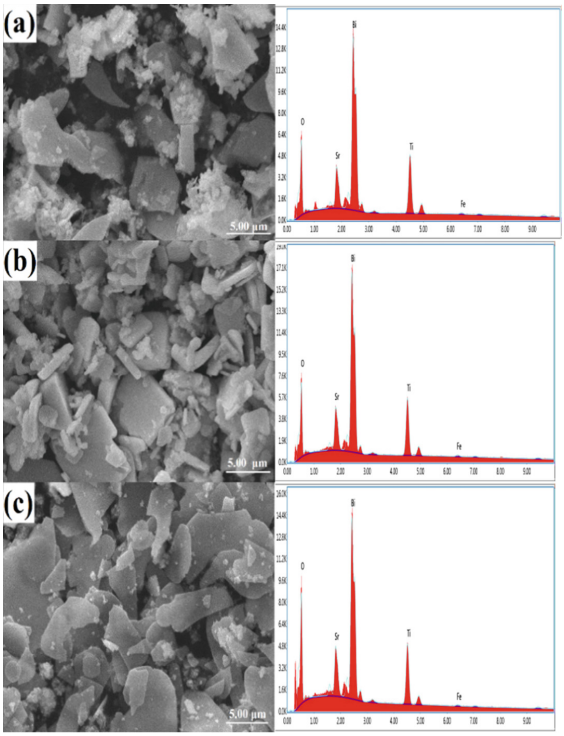

Fig. 4. The micrograph of $SrBi_4Ti_{3.95}Fe_{0.05}O_{15}$ synthesized using (a) NaCl, (b) KCl, dan (c) NaCl/KCl.

Table 2. The percentage of constituent elements of SrBi4Ti3.95Fe0.05O15 compounds

Salt Type	Sr (%)	Bi (%)	Ti (%)	Fe (%)	O (%)
NaCl	7,03	52,53	19,71	1,10	19,61
KCl	7,14	53,95	18,85	1,14	18,91
NaCl/KCl	7,55	49,48	18,02	0,95	24,00

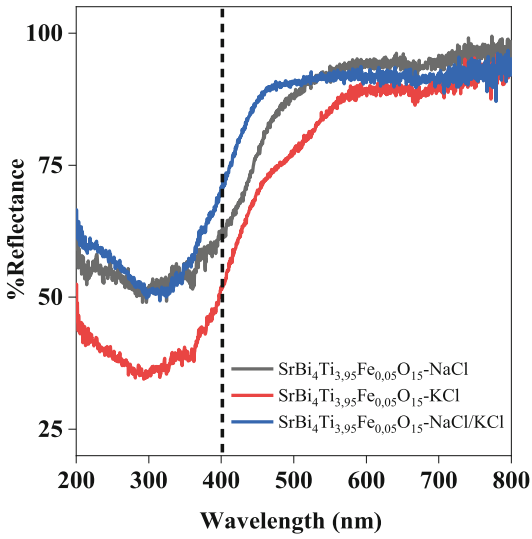

Fig. 5. DRS spectra of $SrBi_4Ti_{3.95}Fe_{0.05}O_{15}$ compound.

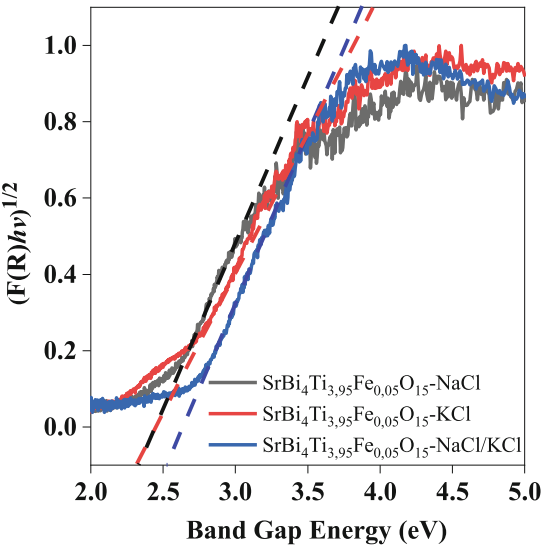

Fig. 6. Plot Tauc of $SrBi_4Ti_{3.95}Fe_{0.05}O_{15}$ compound.

Table 3. The band gap energy of $SrBi_4Ti_{3.95}Fe_{0.05}O_{15}$ compound

Salt Type	Band Gap Energy (eV)	Wavelength (nm)
NaCl	2,34	531
,KCl	2,32	535
NaCl/KCl	2,55	487

4 Conclusion

$SrBi_4Ti_{3.95}Fe_{0.05}O_{15}$ was successfully synthesized using molten salt method with NaCl, KCl, and NaCl/KCl salt. A pure product is formed when using KCl salt with an orthorhombic crystal system and $A2_1am$ space group. An Impurities are still formed when the product synthesized with NaCl and NaCl/KCl salts. It comes from their precursors that are TiO_2 and $SrCO_3$, also it formed a new phase of $Bi_4Ti_3O_{12}$. The product synthesized using KCl salt has more regular plate like shape, meanwhile the product synthesized using NaCl/KCl salt has thinner and elongated particle shape. The different morphology due to the salt type which used in synthesized process.

References

1. Gupta, S.K. & Mao, Y. 2021. A Review On Molten Salt Synthesis of Metal Oxide Nanomaterials: Status, opportunity, and challenge. *Progress in Materials Science*, 117.
2. Tu, S., Zhang, Y., Reshak, A.H., Auluck, S., Ye, L., Han, X., Ma, T. & Huang, H. 2019. Ferroelectric Polarization Promoted Bulk Charge Separation for Highly Efficient CO_2 Photoreduction of $SrBi_4Ti_4O_{15}$. *Nano Energy*, 56: 840–850.
3. Liu, Y., Zhu, G., Gao, J., Hojamberdiev, M., Zhu, R., Wei, X., Guo, Q. & Liu, P. 2017b. Enhanced Photocatalytic Activity of $Bi_4Ti_3O_{12}$ Nanosheets by Fe^{3+}-doping and The Addition of Au Nanoparticles: Photodegradation of Phenol and bisphenol A. *Applied Catalysis B: Environmental*, 200: 72–82.
4. Liu, X., Xu, L., Huang, Y., Qin, C., Qin, L. & Seo, H.J. 2017a. Improved Photochemical Properties of Aurivillius $Bi_5Ti_3FeO_{15}$ With Partial Substitution of Ti^{4+} With Fe^{3+}. *Ceramics International*, 43(15): 12372–12380.
5. He, R., Xu, D., Cheng, B., Yu, J. & Ho, W. 2018. Review on Nanoscale Bi-based Photocatalysts. *Nanoscale Horizons*, 3(5): 464–504.
6. Gu, Y., Yu, F., Chen, J. & Zhang, Q. 2022. Facile Synthesis of Sillén-Aurivillius Layered Oxide $Bi_7Fe_2Ti_2O_{17}Cl$ with Efficient Photocatalytic Performance for Degradation of Tetracycline. *Catalysts*, 12(2): 221.
7. Zulhadjri, Afni, S.E. & Arief, S. 2013. Sintesis Senyawa Aurivillius $SrBi_4Ti_4O_{15}$ yang Didoping Kation La^{3+} Dengan Metode Lelehan Garam. *Prosiding Semirata FMIPA Universitas Lampung*, 489–494.
8. Sari, P., Noerfaiqotul, S., Hardian, A., Aini, N. & Prasetyo, A. 2022. Synthesis and Characterization of Plate-like Vanadium Doped $SrBi_4Ti_4O_{15}$ Prepared via KCl Molten Salt Method. 7(2): 175–180.
9. Kimura, T. 2011. Molten Salt Synthesis of Ceramic Powders. *Advances in Ceramics - Synthesis and Characterization, Processing and Specific Applications.*

10. Chang, Y., Wu, J., Yang, B., Zhang, S., Lv, T. & Cao, W. 2014. Synthesis and Properties of High Aspect Ratio $SrBi_4Ti_4O_{15}$ Microplatelets. *Materials Letters*, 129: 126–129.
11. Liu, R., Zhan, Y., Liu, L., Liu, Y. & Tu, D. 2020. Morphology Analysis and Luminescence Properties of $YVO_4:Sm^{3+},Eu^{3+}$ Prepared by Molten Salt Synthesis. *Optical Materials*, 100: 109633.
12. Safaei-Naeini, Y., Aminzare, M. & Golestani-Fard, F. 2012. The Effects of Temperature and Different Precursors in The Synthesis of Nano Spinel in KCl molten salt. *Ceramics International*, 38(1): 841–845.
13. Meir, R. 2017. Molten Salt Synthesis of Perovskite-Type Oxides Molten Salt Synthesis of Perovskite-Type Oxides.
14. Maulidianingtiyas, H., Prasetiyo, A.D., Haikal, F., Cahyo, I.N., Istighfarini, V.N. & Prasetyo, A. 2021. Pengaruh Penggantian Kation-A/Sr Oleh Ba Pada Morfologi Partikel $Ba_xSr_{(1-x)}TiO_3$ ($x = 0$; 0,2; 0,4; 0,6; 0,8) Hasil Sintesis dengan Metode Lelehan Garam. *ALCHEMY Jurnal Penelitian Kimia*, 17(2): 211.
15. Gu, D., Qin, Y., Wen, Y., Li, T., Qin, L. & Seo, H.J. 2017. Electronic Structure and Optical Properties of V-doped $Bi_4Ti_3O_{12}$ Nanoparticles. *Journal of Alloys and Compounds*, 695: 2224–2231.